J Physiol 596.11 (2018) pp 2131–2146

The Journal of Physiology

A role for focal adhesion kinase in facilitating the contractile responses of murine gastric fundus smooth muscles

Yeming Xie[1], Koon Hee Han[2], Nathan Grainger[1], Wen Li[1], Robert D. Corrigan[1] and Brian A. Perrino[1]

[1] *Department of Physiology and Cell Biology, University of Nevada, Reno, School of Medicine, Reno, NV 89557, USA*
[2] *Department of Internal Medicine, Gangneung Asan Hospital, University of Ulsan College of Medicine, Gangneung, Republic of Korea*

Edited by: Don Bers & Kathleen Morgan

Key points

- Activation of focal adhesion kinase (FAK) by integrin signalling facilitates smooth muscle contraction by transmitting the force generated by myofilament activation to the extracellular matrix and throughout the smooth muscle tissue.
- Here we report that electrical field stimulation (EFS) of cholinergic motor neurons activates FAK in gastric fundus smooth muscles, and that FAK activation by EFS is atropine-sensitive but nicardipine-insensitive. PDBu and calyculin A contracted gastric fundus muscles Ca^{2+}-independently and also activated FAK.
- Inhibition of FAK activation inhibits the contractile responses evoked by EFS, and inhibits CPI-17 phosphorylation at T38.
- This study indicates that mechanical force or tension is sufficient to activate FAK, and that FAK appears to be involved in the activation of the protein kinase C–CPI-17 Ca^{2+} sensitization pathway in gastric fundus smooth muscles.
- These results reveal a novel role for FAK in gastric fundus smooth muscle contraction by facilitating CPI-17 phosphorylation.

Abstract Smooth muscle contraction involves regulating myosin light chain phosphorylation and dephosphorylation by myosin light chain kinase and myosin light chain phosphatase. C-kinase potentiated protein phosphatase-1 inhibitor of 17 kDa (CPI-17) and myosin phosphatase targeting subunit of myosin light-chain phosphatase (MYPT1) are crucial for regulating gastrointestinal smooth muscle contraction by inhibiting myosin light chain phosphatase. Integrin signalling involves the dynamic recruitment of several proteins, including focal adhesion kinase

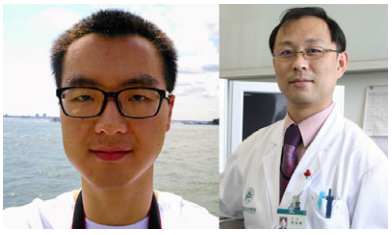

Yeming Xie joined Brian Perrino's group in 2013 and obtained his PhD degree in Cellular & Molecular Pharmacology and Physiology in 2017. He optimized an automated capillary electrophoresis and western blot approach, and an *in situ* proximity ligation assay to study murine and human gastric fundus protein phosphorylation and protein–protein interactions. His research revealed a novel role for focal adhesion kinase in regulating gastric fundus smooth muscle contraction. He is currently a post-doctoral scientist in the laboratory of Wei Yan, studying spermatogenesis using next-generation sequencing technologies. **Koon Hee Han** received his MD from the Chungnam National University in 2001, and his PhD in Physiology from the Catholic Kwandong University of South Korea in 2011. He did resident and fellowship training at Gangneung Asan Hospital. He is currently an Associate Professor, Division of Gastroenterology, Ulsan University College of Medicine, in Gangneung. His research interests focus on smooth muscle motility and inflammatory bowel disease.

Y. Xie and K. H. Han are co-first authors.

DOI: 10.1113/JP275406

(FAK), to focal adhesions. FAK tyrosine kinase activation is involved in cell adhesion to the extracellular matrix via integrin signalling. FAK participates in linking the force generated by myofilament activation to the extracellular matrix and throughout the smooth muscle tissue. Here, we show that cholinergic stimulation activates FAK in gastric fundus smooth muscles. Electrical field stimulation in the presence of N^{ω}-nitro-L-arginine methyl ester and MRS2500 contracted gastric fundus smooth muscle strips and increased FAK Y397 phosphorylation (pY397). Atropine blocked the contractions and prevented the increase in pY397. The FAK inhibitor PF-431396 inhibited the contractions and the increase in pY397. PF-431396 also inhibited the electrical field stimulation-induced increase in CPI-17 T38 phosphorylation, and reduced MYPT1 T696 and T853, and myosin light chain S19 phosphorylation. Ca^{2+} influx was unaffected by PF-431396. Nicardipine inhibited the contractions but had no effect on the increase in pY397. Phorbol 12,13-dibutyrate or calyculin A contracted gastric fundus smooth muscle strips Ca^{2+} independently and increased pY397. Our findings suggest that FAK is activated by mechanical forces during contraction and reveal a novel role of FAK in the regulation of CPI-17 phosphorylation.

(Resubmitted 7 February 2018; accepted after revision 26 February 2018; first published online 12 March 2018)
Corresponding author B. A. Perrino: University of Nevada Reno School of Medicine, 1664 N Virginia St. MS0352, Reno, NV 89557, USA. Email: bperrino@med.unr.edu

Introduction

The trigger for contraction of gastrointestinal smooth muscles is a rapid increase in intracellular Ca^{2+} $[Ca^{2+}]_i$. Membrane depolarization evokes the opening of voltage-dependent (L-type) Ca^{2+} channels, non-selective cation currents, and other mechanisms that contribute to the Ca^{2+} influx and the increase in $[Ca^{2+}]_i$ (Sanders *et al.* 2012; Chen *et al.* 2015). The increase in $[Ca^{2+}]_i$ activates the calmodulin-dependent myosin light chain kinase, which phosphorylates myosin light chain (MYL9) at S19 (pS19), stimulating myosin ATPase activity to generate cross-bridge cycling and contraction (He *et al.* 2008; Mizuno *et al.* 2008). Termination of the contractile signal leads to a decrease in $[Ca^{2+}]_i$, and inactivation of myosin light chain kinase. MYL9 is then dephosphorylated by myosin light chain phosphatase (MLCP), leading to relaxation (Somlyo & Somlyo, 2003). Numerous reports show that a common mechanism regulating S19 phosphorylation involves inhibition of MLCP by protein kinase C (PKC)-mediated phosphorylation of C-kinase potentiated protein phosphatase-1 inhibitor of 17 kDa (CPI-17) at T38 (pT38) and/or phosphorylation of myosin phosphatase targeting subunit of MLCP (MYPT1) by Rho-associated kinase 2 (ROCK2) (Hirano, 2007). MYPT1 phosphorylation at T696 (pT696) and/or T853 (pT853) (human isoform numbering) inhibits MLCP activity, but pT853 does not appear to inhibit MLCP *in vivo* (Hartshorne *et al.* 2004; He *et al.* 2008; Matsumura & Hartshorne, 2008; Grassie *et al.* 2011; Khasnis *et al.* 2014; Chen *et al.* 2015). However, ROCK2 activity, as indicated by MYPT1 T853 phosphorylation, is clearly required for Ca^{2+} sensitization and augmented contraction (Chen *et al.* 2015).

In addition to Ca^{2+}-dependent myofilament activation and Ca^{2+} sensitization by inhibition of MLCP, a number of studies have provided evidence that dynamic changes to the actin cytoskeleton play an important role in smooth muscle contraction (Mehta & Gunst, 1999; Kunit *et al.* 2014; Mills *et al.* 2015*a*). Tyrosine phosphorylation of protein tyrosine kinase 2 β (Pyk2) and focal adhesion kinase (FAK), along with the recruitment of other integrin-associated proteins to focal adhesions, occurs during contraction and force development (Mehta & Gunst, 1999; Chen *et al.* 2015; Mills *et al.* 2015*b*). This remodelling process is thought to facilitate the polymerization of cortical cytoskeletal actin filaments to increase the stability of focal adhesions in the membrane, allowing for the force generated by myofilament activation to be transmitted to the connective tissue of the extracellular matrix (Mehta & Gunst, 1999; Chen *et al.* 2015; Mills *et al.* 2015*b*).

In gastric fundus smooth muscles, we previously found that electrical field stimulation (EFS)-evoked contractions increase CPI-17, but not MYPT1, phosphorylation, and that PKC inhibitors block the increase in CPI-17 phosphorylation and the increase in contraction (Bhetwal *et al.* 2013). The involvement of FAK and Pyk2 in facilitating smooth muscle contractile responses has previously been studied in various smooth muscle tissues including airway, vascular, bladder and prostate smooth muscle (Mehta & Gunst, 1999; Kunit *et al.* 2014; Chen *et al.* 2015; Mills *et al.* 2015*a*). The Ca^{2+}-dependent tyrosine kinase Pyk2 has been reported to be activated by

membrane depolarization and voltage-dependent Ca^{2+} influx resulting in RhoA activation leading to MYPT1 and MYL9 phosphorylation and MLCP inhibition in vascular smooth muscles, while FAK Y397 phosphorylation has been shown to be increased during bladder smooth muscle contraction (Luo *et al.* 2013; Chen *et al.* 2015; Mills *et al.* 2015*a*). These findings suggesting that either Pyk2 or FAK may play a role in the contractile responses of different smooth muscles. No studies have addressed the roles of Pyk2 or FAK in gastrointestinal smooth muscles. Thus, in this study we investigated the role of FAK and Pyk2 in regulating GI smooth muscle contractility, and show that FAK activation facilitates gastric fundus smooth muscle contraction.

Methods

Ethical approval

Male C57BL/6 mice were purchased from Charles River Laboratories (Hollister, CA, USA). GCaMP3-floxed mice (B6.129S-*Gt(ROSA)26Sor*$^{tm38(CAG\text{-}GCaMP3)Hze}$/J) and SMMHC-Cre mice (B6.FVB-Tg Myh11-cre/ER^{T2}) were purchased from The Jackson Laboratory (Sacramento, CA, USA). These mice were crossed to produce SMMHC-Cre-GCaMP3 mice which exclusively express the fluorescent reporter GCaMP3 in smooth muscle myosin heavy chain (SMMHC)-positive cells. SMMHC-Cre-GCaMP3 mice aged between 6 and 8 weeks of age were then injected with tamoxifen (2 mg for three consecutive days) as described previously (Baker *et al.* 2016). Mice were genotyped 10 days following the initial injection to confirm stop codon excision and subsequent expression of GCaMP3. The mice were maintained and experiments carried out according to the National Institutes of Health *Guide for the Care and Use of Laboratory Animals*. Animal protocols were approved by the University of Nevada, Reno, Institutional Animal Care and Use Committee. Mice were housed in a pathogen-free facility with a 12 h light/dark cycle and free access to water and food (Prolab 5P76 Isopro 3000; 5.4% fat by weight). Our methods comply with the animal ethics checklist outlined in *The Journal of Physiology* (Grundy, 2015).

Tissue preparation

Mice were anaesthetized by isoflurane inhalation and killed by decapitation. Livers were removed, rinsed with Krebs–Ringer buffer, flash-frozen in liquid N_2 and stored at −80°C. The stomachs were removed, pinned to a Sylgard-lined dish and placed in 4°C oxygenated (97% O_2–3% CO_2) Krebs–Ringer buffer. The mucosa and submucosa were removed from the gastric fundus by sharp dissection (Kim *et al.* 2005). The smooth muscles were pre-equilibrated for 45 min in 37°C oxygenated Krebs–Ringer buffer before use for tension measurements.

Mechanical responses

Contractile activity was measured in static myobaths (Bhetwal *et al.* 2013). Gastric fundus smooth muscle strips (∼10 mm × 2 mm) were attached to a Fort 10 isometric strain gauge (WPI, Sarasota, FL, USA), in parallel with the circular muscles (Kim *et al.* 2005). Each muscle strip was equilibrated in 37°C oxygenated Krebs–Ringer buffer for 1 h. To measure contractile responses to cholinergic neurotransmission, muscle strips were incubated with 100 μM N^{ω}-nitro-L-arginine methyl ester (L-NAME) and 1 μM MRS2500 (to inhibit nitrergic and purinergic inhibitory motor neurons) prior to the delivery of square-wave pulses of EFS (0.3 ms duration), 150 V, 30 s duration (supra-maximal voltage; Grass S48 stimulator, West Warwick RI, USA) (Bhetwal *et al.* 2013). To measure contractile responses to KCl, phorbol 12,13-dibutyrate (PDBu), or calyculin A, the muscle strips were incubated with 0.3 μM tetrodotoxin to eliminate all motor neuron activity. Muscle responses were recorded and analysed with Acqknowledge 3.2.7 software (BIOPAC Systems, Goleta, CA, USA). For Wes Simple Western analysis of proteins (see later), the myobath chamber was quickly dropped down and the tissue rapidly immersed into ice-cold acetone, 10 mM dithiothreitol (DTT), 10% (w/v) trichloroacetic acid (TCA) for 1 min. During EFS, the stimulation was on while dropping the bath down and submerging the tissue into the ice-cold acetone–DTT–TCA (Bhetwal *et al.* 2013). The tissues were then snap-frozen in liquid N_2, and stored at −80°C (Bhetwal *et al.* 2011).

Ca^{2+} imaging

Each gastric fundus muscle preparation was equilibrated by perfusion (1.6 ml min^{-1}) with oxygenated Krebs–Ringer buffer for 45 min at 37°C. To visualize Ca^{2+} transients, fundus muscles from C57/BL6 mice were incubated in Ca^{2+} physiological salt solution (PSS) containing 10 μM Cal-520 AM (AAT Bio-quest, Sunnyvale, CA, USA) and cremophor EL (0.01%, Sigma-Aldrich, St Louis, MO, USA) for 15 min at room temperature, followed by de-esterification for 20 min at room temperature. Following incubation, the recording chamber was mounted on the stage of a wide-zoom stereo microscope (SZX16; Olympus Corporation, Waltham, MA, USA), and visualized and imaged using magnifications from ×2 to ×10. The preparations were superfused with dye-free PSS, illuminated at 488 nm using dichroic mirrors and an Olympus light source (Olympus U-LH100HGAPO), and fluorescence emissions at 520 nm were captured through a barrier filter. Experiments were performed by applying electrical field stimulation (10 Hz for 10 s) in the presence of 100 μM L-NAME and 1 μM MRS2500 before and after adding PF-431396 (300 nM), along with unstimulated, control

recordings in the absence and presence of PF-431396. Solutions containing PF-431396 were perfused into the chamber for 15 min to allow full tissue penetration. Gastric fundus muscles from SMMHC-Cre-GCaMP3 mice were perfused (2 ml min^{-1}) with oxygenated Krebs–Ringer buffer solution at 37°C and then allowed to equilibrate for 1 h. Preparations were visualized and imaged using an upright Nikon Eclipse E600FN microscope using a ×4 Plan Fluor lens (Nikon, Edgewood, NY, USA). Each gastric fundus muscle was incubated with 60 mM KCl, followed by washout, followed by incubation with PdBu, and then washout and then incubation with calyculin A. Images were acquired using a high-speed sCMOS camera (Andor Neo sCMOS, Andor Technology, Belfast, UK). Image sequences were sampled at 6.24 Hz using Andor Solis software. The GCaMP3 fluorophore was excited at 488 nm using a B-2E/C dichroic mirror (excitation filter wavelength: 465–495 nm) and an LED Sola Light Engine (Lumencor, Beaverton, OR, USA), and fluorescence emissions at 520 nm captured through a barrier filter (emission filter wavelength: 515–555 nm). After acquisition, image sequences were analysed using open-source Fiji software (Schindelin *et al.* 2012). Images were first converted to 32-bit format and background fluorescence signal removed from image sequences by sampling greyscale pixel intensities and subtracting minimum intensity values from the images. Linescans were drawn over areas perpendicular to the smooth muscle and the reslice function performed to generate a spatiotemporal (ST) map. Basal fluorescence (F_0) was calculated from the ST maps by analysing the pixel intensities prior to pharmacological intervention. F/F_0 was calculated by dividing the F_0 value from the entire ST map. Single image frames were taken at the beginning of the recording period, prior to pharmacological application and at time point deemed to be the peak of contraction (maximum tissue distortion). The amplitudes of the Ca^{2+} transients are expressed as the F/F_0 average pixel intensity or intensity units (iu) to generate the traces of calcium activity.

Automated capillary electrophoresis and immunoblotting with Wes Simple Western

Muscles were washed in ice-cold-acetone–10 mM DTT for 1 min, 3 times, followed by a 1 min wash in ice-cold lysis buffer (mM: 50 Tris–HCl pH 8.0, 60 β-glycerophosphate, 100 NaF, 2 EGTA, 25 sodium pyrophosphate, 1 DTT, 0.5% NP-40, 0.2% sodium dodecyl sulfate and protease inhibitors (Bhetwal *et al.* 2011). Tissues were homogenized in 0.3 ml lysis buffer in a Bullet Blender (0.01% anti-foam C, one stainless steel bead per tube, speed 6, 5 min), then centrifuged at 16,000 *g*, 10 min and 4°C. Supernatants were stored at −80°C. Protein concentrations of the supernatants were determined by the Bradford assay using bovine γ-globulin as the standard. Protein expression and phosphorylation levels were measured and analysed according to the Wes User Guide using a Wes Simple Western instrument from ProteinSimple (San Jose, CA, USA). The protein samples were mixed with the fluorescent 5× master mix (ProteinSimple) and then heated at 95°C for 5 min. Boiled samples, biotinylated protein ladder, blocking buffer, primary antibodies, ProteinSimple horseradish peroxidase-conjugated anti-rabbit or anti-mouse secondary antibodies, luminol-peroxide and wash buffer were loaded into the Wes plate (Wes 12–230 kDa Pre-filled Plates with Split Buffer, ProteinSimple). The plates and capillary cartridges were loaded into the Wes instrument, and protein separation, antibody incubation and imaging were performed using default parameters. Compass software (ProteinSimple) was used to acquire the data, and to generate image reconstruction and chemiluminescence signal intensities. The protein and phosphorylation levels are expressed as the area of the peak chemiluminescence intensity. The following primary antibodies were used: mouse anti-CPI-17 (PPP1R14A) (sc-48406; 1:200), rabbit anti-pT38-CPI-17 (sc-17560; 1:200), rabbit anti-MYL9 (sc-15370; 1:400), rabbit anti-pS19-MYL9 (sc-12896; 1:200), rabbit anti-MYPT1 (PPP1R12A) (sc-25618; 1:200), rabbit anti-pT696-MYPT1 (sc-17556-R; 1:200), rabbit anti-pT853-MYPT1 (sc-17432-R; 1:200), rabbit anti-Pyk2 (Ptk2b) (sc-9019; 1:200), rabbit anti-pT402-Pyk2 (sc-11767-R; 1:200) (Santa Cruz Biotechnology, Dallas, TX, USA); and rabbit anti-FAK (no. 3281; 1:100) and rabbit anti-pY397-FAK (no. 8556; 1:100) (Cell Signaling Technology, Danvers, MA, USA).

Data and statistical analysis

The area of the peak chemiluminescence intensity values of the protein bands were calculated by Compass software. The chemiluminescence intensity values of pT853, pT38, pS19, pY397 and pY402 were divided by the total MYPT1, CPI-17, MYL9, FAK and Pyk2 chemiluminescence intensity values from the same sample, respectively, to obtain the ratio of phosphorylated protein to total protein. The ratios were normalized to 1 for unstimulated muscles (Control, basal levels), and all ratios were subsequently analysed by non-parametric repeated tests of ANOVA using Prism 7.01 software (GraphPad Software, San Diego, CA, USA), and are expressed as the means ± SD. Student's *t* test was used to measure significance and $P < 0.05$ is considered significant. The digital lane views (bitmaps) of the immunodetected protein bands were generated by Compass software, with each lane corresponding to an individual capillary tube. The immunodetection figures were created from the digitized data using Adobe Photoshop Version: 12.0.3. Contractile responses were compared by measuring the maximum height of each peak (g), and

the area under the curve (AUC) of each peak including the contribution of basal tone (integral, grams × seconds) divided by time (seconds), per cross-sectional area (cm^2) of the smooth muscles, using Acknowledge. The average peak responses (mean (SD)) were calculated using Prism, and significance was determined by *t* test using Prism with $P < 0.05$ considered as significant. Graphs were generated using Prism.

Drugs and reagents

Atropine and tetrodotoxin were obtained from EMD Millipore (Billerica, MA, USA), L-NAME and PF-431396 were obtained from Sigma-Aldrich, and MRS2500 and FAK Inhibitor 14 (FI14) were purchased from Tocris Bioscience (Bristol, UK). All other reagents and chemicals purchased were of analytical grade or better. PF-431396 and FI14 were dissolved in dimethyl sulfoxide (DMSO) and then diluted to the indicated final concentrations.

Results

EFS of cholinergic motor neurons increases FAK Y397 phosphorylation

As noted previously, FAK and Pyk2 autophosphorylation have both been reported to be involved in the contraction of smooth muscles. To determine whether FAK and Pyk2 are activated in response to cholinergic stimulation in gastric fundus smooth muscles, we measured FAK and Pyk2 phosphorylation during EFS-evoked contractions. As we previously reported with 10 Hz stimulation, the peak of contraction occurred at 5 s (Fig. 1*A*) (Bhetwal *et al.* 2013), with an average maximum force generation of 0.143 ± 0.024 g (Fig. 1*B*). FAK and Pyk2 phosphorylation were measured from unstimulated muscle strips, and at the 5 s peak of contraction (Fig. 1*C* and *E*). There is a basal level of Y397 phosphorylation that was increased 1.73 ± 0.35-fold by EFS (Fig. 1*D*). In contrast to FAK, there was no detectable Pyk2 phosphorylation in control or EFS stimulated fundus smooth muscles (Fig. 1*E* and *F*). Liver homogenates were used as positive controls for the immunodetection of phosphorylated Pyk2 (Fig. 1*E*) (Yu *et al.* 2005). Thus, we investigated FAK phosphorylation during EFS-induced cholinergic stimulation of gastric fundus smooth muscles.

Effect of the FAK inhibitor PF-431396 on basal tone and FAK Y397 phosphorylation

PF-431396 has previously been used to inhibit FAK phosphorylation (Saphirstein *et al.* 2013; Chien *et al.* 2015). To investigate the effect of inhibiting Y397 phosphorylation on contraction, we determined the concentration-dependent effects of PF-431396 on FAK Y397 phosphorylation and fundus smooth muscle basal tone. Fundus muscle strips showed little to no change in basal tone when treated with vehicle, 0.1 or 0.3 μM PF-431396 (Fig. 2*A* and *B*). However, basal tone was reduced by 1 μM PF-431396 (0.028 ± 0.006 g reduced tone) and 3 μM PF-431396 (0.097 ± 0.008 g reduced tone) (Fig. 2*A* and *B*). FAK Y397 autophosphorylation was inhibited at each concentration of PF-431396 (Fig. 2*C* and *D*). We chose 0.3 μM PF-431396 for this study since the inhibition of FAK Y397 phosphorylation was nearly maximal at 0.3 μM PF-431396, with no reduction in basal tone.

PF-431396 inhibits FAK Y397 phosphorylation and EFS-evoked contraction

Incubation of gastric fundus smooth muscle strips with 0.3 μM PF-431396 markedly inhibited EFS-induced contractions (Fig. 3*A* and *B*). As measured by the integral of contraction, the contractile responses to 5, 10 and 20 Hz EFS were significantly inhibited by 0.3 μM PF-431396 (65.1 ± 11.3%, 64.8 ± 11.6% and 53.9 ± 20.5% inhibition, respectively). The 10 Hz, 5 s EFS-induced increase in pY397 was blocked by 0.3 μM PF-431396 (Fig. 3*C* and *D*). The levels of pY397 were increased almost twofold by EFS (1.731 ± 0.203-fold), but in the presence of PF-431396, the pY397 levels were reduced below the basal, control levels (Fig. 3*C* and *D*).

Atropine inhibits EFS-induced FAK Y397 phosphorylation

To determine that FAK activation and inhibition of FAK activation is occurring in post-junctional cells, we investigated the effects of atropine on the EFS-induced increase in pY397. Atropine completely blocked the EFS-evoked contractile responses (Fig. 4*A* and *B*), and the increase in pY397 evoked by 10 Hz, 5 s EFS (Fig. 4*C* and *D*), indicating that FAK is activated in post-junctional cells by EFS-induced cholinergic neurotransmission.

PF-431396 inhibits high K^+-evoked contraction and FAK Y397 phosphorylation

To further show that FAK activation and inhibition of FAK activation occurs in smooth muscle cells we determined the effects of high K^+-induced contraction on FAK Y397 phosphorylation. High extracellular K^+ (33 mM) contracted gastric fundus smooth muscle strips, with a maximal force generation of 0.352 ± 0.064 g (Fig. 5*A*). No difference in contraction was observed between high K^+ pre-stimulation and the subsequent high K^+ stimulation, in which 0.1% DMSO was applied as the vehicle (Fig. 5*A*). Thus, we could compare PF-431396 inhibition of high K^+ stimulated contraction to the high K^+ pre-stimulation

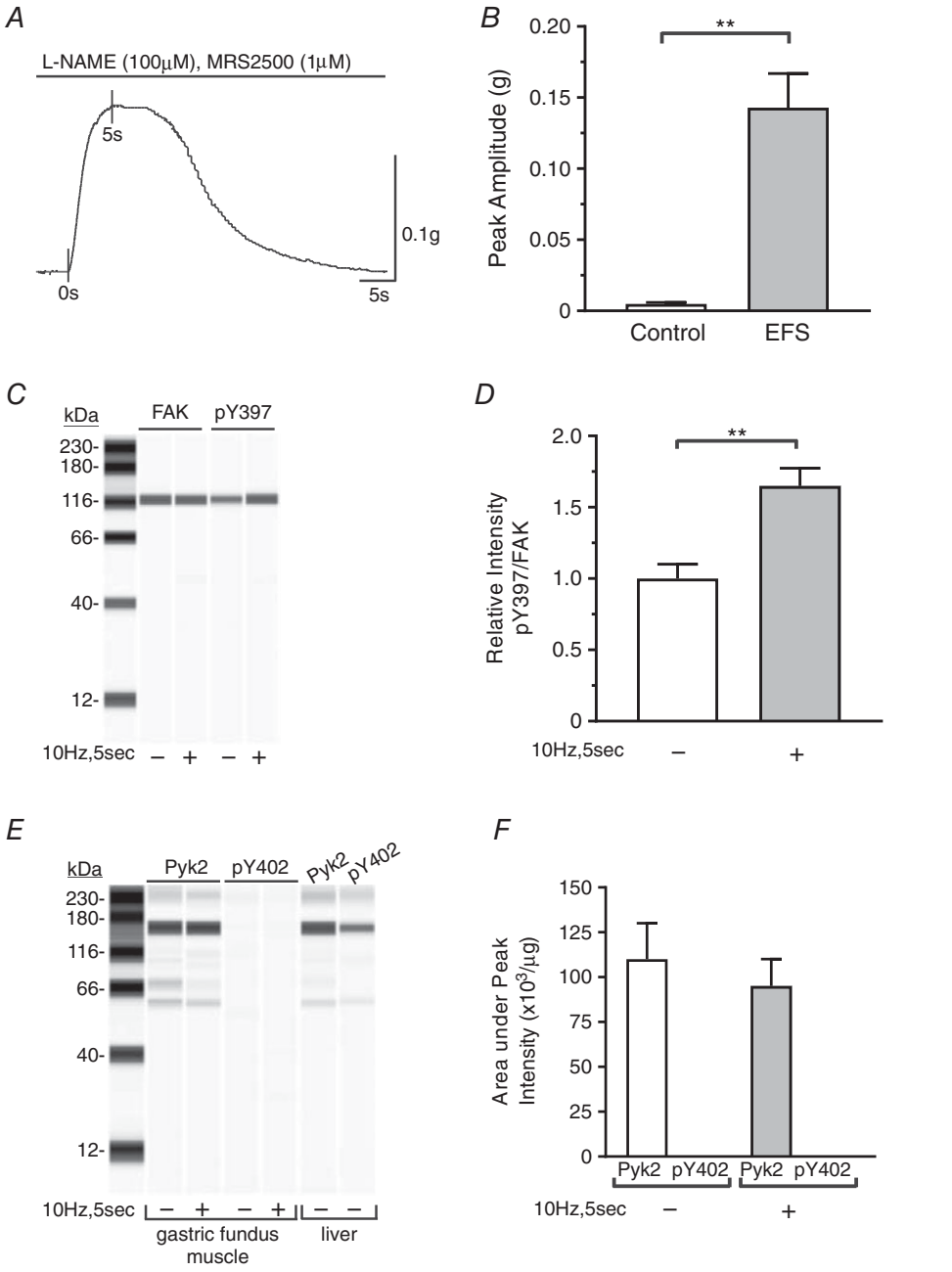

Figure 1. EFS induces phosphorylation of FAK but not Pyk2 during gastric fundus smooth muscle contraction

A, representative trace of muscle strip contractions in response to 10 Hz EFS in the presence of 100 μM L-NAME and 1 μM MRS2500. FAK and Pyk2 phosphorylation were measured at the 5 s time point. *B*, the mean ± SD of the amplitude of contraction evoked by 10 Hz EFS at 5 s ($n = 6$). $^{**}P < 0.01$. *C*, representative immunoblot of FAK and pY397 from unstimulated and 10 Hz, 5 s EFS fundus muscles; 0.5 μg per lane. *D*, mean ± SD of the pY397:FAK area under the peak intensity ratios from unstimulated and 10 Hz, 5 s EFS fundus muscles ($n = 3$). $^{**}P < 0.01$. *E*, representative immunoblot of Pyk2 and pY402 from liver, and from unstimulated and 10 Hz, 5 s EFS fundus smooth muscles; 1.0 μg per lane. *F*, mean ± SD of the Pyk2 and pY402 area under the peak intensity per μg lysate protein from unstimulated and 10 Hz, 5 s EFS fundus muscles ($n = 3$).

contraction in the same smooth muscle strip. PF-431396 (0.3 μM) inhibited the high K^+-induced contractions by 39.8 ± 7.5% (Fig. 5*B*). High K^+ also induced a 25 ± 3.2% increase in pY397, which was blocked by 0.3 μM PF-431396, further showing that FAK is activated in fundus smooth muscle cells (Fig. 5*C* and *D*).

Effects of PF-431396 on CPI-17, MYPT1 and MYL9 phosphorylation evoked by EFS

Inhibition of the Ca^{2+}-stimulated protein tyrosine kinase Pyk2 inhibits RhoA activation, and MYPT1 and MYL9 phosphorylation in caudal artery smooth muscle cells (Mills *et al.* 2015*a*).We previously reported that EFS-evoked cholinergic neurotransmission increases CPI-17 phosphorylation (Bhetwal *et al.* 2013). Thus, to determine if gastric fundus muscle Ca^{2+} sensitization pathways are modulated by FAK activation, we examined the effects of PF-431396 on Ca^{2+} sensitization protein phosphorylation. As expected, 10 Hz, 5 s EFS significantly increased the CPI-17 pT38 levels, by 3.5 ± 0.068-fold, and this increase was blocked by PF-431396 (Fig. 6*A* and *B*). The MYPT1 pT853 levels were not significantly increased by 10 Hz, 5 s EFS, but PF-431396 decreased the pT853 levels in muscles treated with PF-431396 during EFS, compared to EFS alone (Fig. 6*C* and *D*). In addition, as expected, EFS did not increase the pMYPT1 T696 levels, but PF-431396 decreased the pT696 levels below the basal levels by 30 ± 3.1% (Fig. 6*E* and *F*). The bands below the pT696 bands are likely due to phosphorylated T560 of MBS85, which shares significant sequence identity with sequence of MYPT1 surrounding pT696 (Grassie *et al.* 2011). MBS85 is an MYPT1 family member, expressed in smooth muscles; but at fairly lower levels relative to MYPT1 (Tsai *et al.* 2014). It also regulates myosin phosphatase activity: when T560 is phosphorylated, MBS85 interacts with PP1cδ and inhibits myosin light chain phosphatase activity (Grassie *et al.* 2011). Finally, MYL9 phosphorylation at S19 was not significantly increased by 10 Hz, 5 s EFS, but in the presence of PF-431396 during EFS, the pS19 levels were reduced by 64 ± 1% compared to the control levels (Fig. 6*G* and *H*).

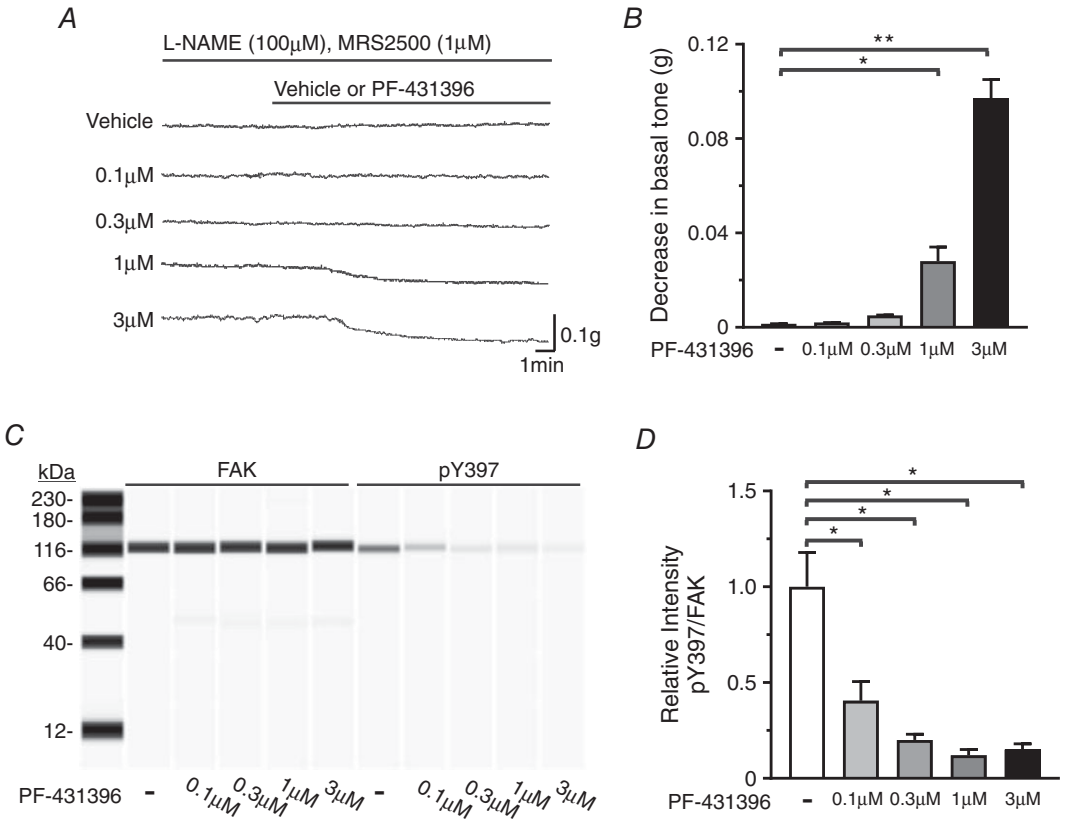

Figure 2. Dose–response of PF-431396 on basal tone and FAK Y397 phosphorylation
A, representative traces of gastric fundus smooth muscle basal tones without or with vehicle, 0.1, 0.3, 1 or 3 μM PF-431396 in the presence of 100 μM L-NAME and 1 μM MRS2500. *B*, mean ± SD of the change in basal tone amplitudes in response to vehicle, 0.1, 0.3, 1 or 3 μM PF-431396 (*$P < 0.05$, **$P < 0.01$, $n = 3$, each treatment). *C*, representative immunoblot of FAK and pY397 in the absence or presence of increasing concentrations of PF-431396; 0.5 μg per lane. *D*, mean ratios ± SD of pY397:FAK in the absence or presence of increasing concentrations of PF-431396 (*$P < 0.05$, $n = 3$, each treatment).

PF-431396 does not inhibit EFS-evoked Ca^{2+} influx into smooth muscle cells

We examined the effect of PF-431396 on EFS-evoked Ca^{2+} influx because the above findings could also be due to inhibition of Ca^{2+} influx by tyrosine kinase inhibition, or by off-target inhibition by PF-431396 (Katsube *et al.* 1998; Son *et al.* 2013). Gastric fundus smooth muscles were loaded with the fluorescent Ca^{2+} indicator dye Cal-520, and then stimulated with 10 Hz for 10 s in the absence or presence of 0.3 μM PF-431396. As expected, 10 Hz, 10 s EFS

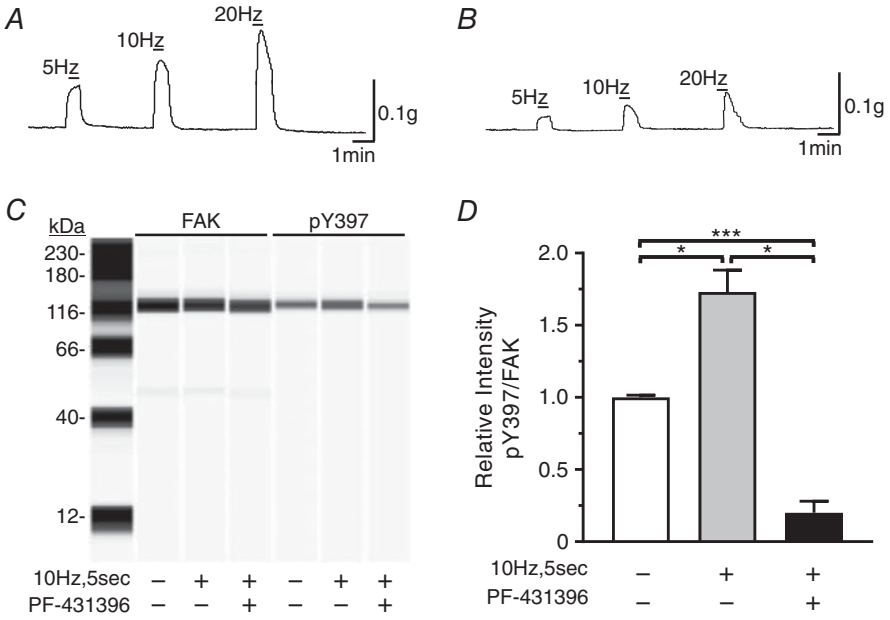

Figure 3. PF-431396 inhibits EFS-induced contractile responses and FAK Y397 phosphorylation
A and *B*, representative traces of the contractile response of gastric fundus smooth muscles to 30 s of 5, 10 or 20 Hz EFS without (*A*) or with (*B*) 0.3 μM PF-431396 in the presence of 100 μM L-NAME and 1 μM MRS2500 ($n = 3$). *C*, representative immunoblot of FAK and pY397 in unstimulated muscles, and muscles contracted with 10 Hz, 5 s EFS without or with 0.3 μM PF-431396, in the presence of 100 μM L-NAME and 1 μM MRS2500; 0.5 μg per lane. *D*, mean ratios ± SD of pY397:FAK from unstimulated muscles, and muscles contracted with 10 Hz, 5 s EFS without or with 0.3 μM PF-431396. $^*P < 0.05$, $^{***}P < 0.005$, $n = 3$.

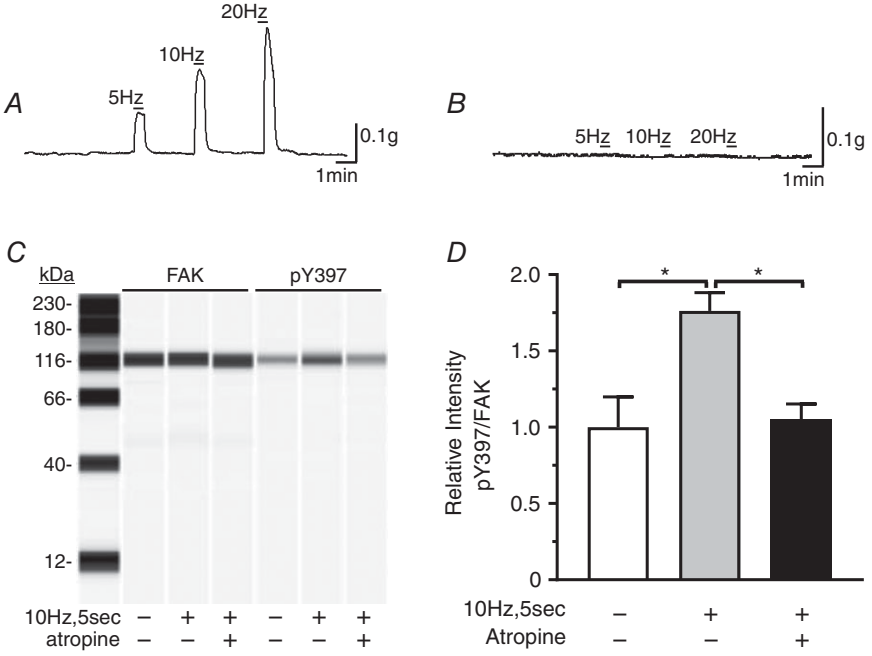

Figure 4. Atropine blocks EFS-induced contractile responses and the EFS-induced increase in FAK phosphorylation
A and *B*, representative traces of the contractile response of gastric fundus smooth muscles to 30 s of 5, 10 or 20 Hz EFS without (*A*) or with (*B*) 1 μM atropine in the presence of 100 μM L-NAME and 1 μM MRS2500 ($n = 3$). *C*, representative immunoblot of FAK and pY397 from unstimulated and 10 Hz, 5 s EFS muscles in the absence or presence of 1 μM atropine; 0.5 μg per lane. *D*, the mean ± SD of pY397:FAK area under the peak intensity ratios from unstimulated and 10 Hz, 5 s EFS muscles in the absence or presence of 1 μM atropine ($n = 3$). $^*P < 0.05$.

evoked a robust Ca^{2+} influx, as indicated by the increase in fluorescence intensity (Fig. 7*A*, *C* and *E*). Similar increases in fluorescence intensity were evoked by 10 Hz, 10 s EFS in the presence of 0.3 μM PF-431396 (Fig. 7*B*, *D* and *E*), indicating that PF-431396 had no effect on EFS-evoked Ca^{2+} influx.

Nicardipine does not inhibit the EFS-evoked increase in FAK pY397

We examined the effects of nicardipine on the EFS-evoked increase in pY397 to determine whether Ca^{2+} influx contributes to the increase in FAK pY397. As expected, the EFS-evoked contractions (Fig. 8*A*) were markedly inhibited by 1 μM nicardipine (Fig. 8*B*). As measured by the integral of contraction, the contractile responses to 5, 10 and 20 Hz EFS were inhibited by 70.1 ± 2.3%, 73.1 ± 1.8% and 72.6 ± 3.1%, respectively. In contrast, 1 μM nicardipine had no effect on the increase in pY397 evoked by 10 Hz, 5 s EFS (Fig. 8*C* and *E*), suggesting that Ca^{2+} influx is not required for the EFS-evoked increase in FAK pY397.

PDBu and calyculin A contract gastric fundus smooth muscles Ca^{2+}-independently

Although PDBu and calyculin A have been shown to contract smooth muscles in a Ca^{2+}-independent manner the Ca^{2+}-independent contraction of gastric fundus muscles by PDBu or calyculin A has not been reported (Ishihara *et al.* 1989; Horowitz *et al.* 1996; Throckmorton *et al.* 1998). Thus, we used PDBu and calyculin A to determine whether FAK activation during gastric fundus smooth contraction occurs Ca^{2+}-independently. We used gastric fundus smooth muscles from SMMHC-Cre-GCaMP3 mice, which express the Ca^{2+} indicator GCaMP3 specifically in smooth muscle cells (Baker *et al.* 2016). Figure 9*A–C* shows that 0.5 μM PDBu contracted gastric fundus smooth muscle strips from GCaMP mice, without a corresponding increase in cytosolic Ca^{2+}. Similarly, Fig. 9*D–F* shows that 0.5 μM calyculin A also contracted gastric fundus smooth muscle strips from GCaMP mice without a corresponding increase in cytosolic Ca^{2+}. Although the times to achieve maximum force were slower than EFS-evoked contractions, the maximum force generated by each compound was similar to the maximum force generated by 20 Hz EFS. We used 60 mM extracellular KCl as a positive control to show that Ca^{2+} influx evokes a strong fluorescence signal from GCaMP gastric fundus smooth muscles (Fig. 9*G* and *H*).

PDBu and calyculin A increase FAK Y397 phosphorylation

FAK Y397 phosphorylation was measured from unstimulated fundus muscle strips, and from gastric fundus muscle strips contracted by 0.5 μM PDBu or 0.5 μM calyculin A for 2 min. As shown in Fig. 10, PDBu (Fig. 10*A* and *B*) or calyculin A (Fig. 10*C* and *D*) significantly increased FAK Y397 phosphorylation, supporting the conclusions that mechanical stimulation or tension is sufficient to increase FAK pY397, and that Ca^{2+} influx is not required for the increase in FAK pY397 evoked by contraction.

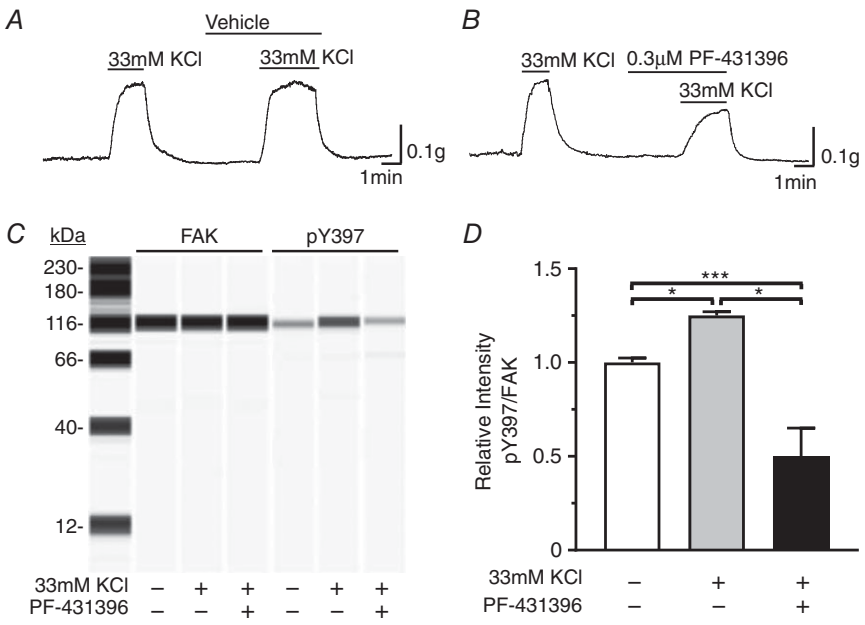

Figure 5. PF-431396 inhibits high K^+-evoked contractions and FAK Y397 autophosphorylation
A, representative trace of the contractile response of gastric fundus smooth muscles to 33 mM KCl without and with vehicle (0.1% DMSO) ($n = 3$). *B*, representative trace of the contractile responses to 33 mM KCl without and with 0.3 μM PF-431396 ($n = 3$). Tetrodotoxin at 0.3 μM was present in the myobath. *C*, representative immunoblot of FAK and pY397 from unstimulated and 33 mM KCl stimulated muscles in the absence or presence of 0.3 μM PF-431396; 0.5 μg per lane. *D*, the mean ratios ± SD of pY397:FAK area under the peak intensity ratios from unstimulated muscles and muscles contracted with 33 mM KCl in the absence or presence of 0.3 μM PF-431396 ($n = 3$, each treatment). $^*P < 0.05$, $^{***}P < 0.005$.

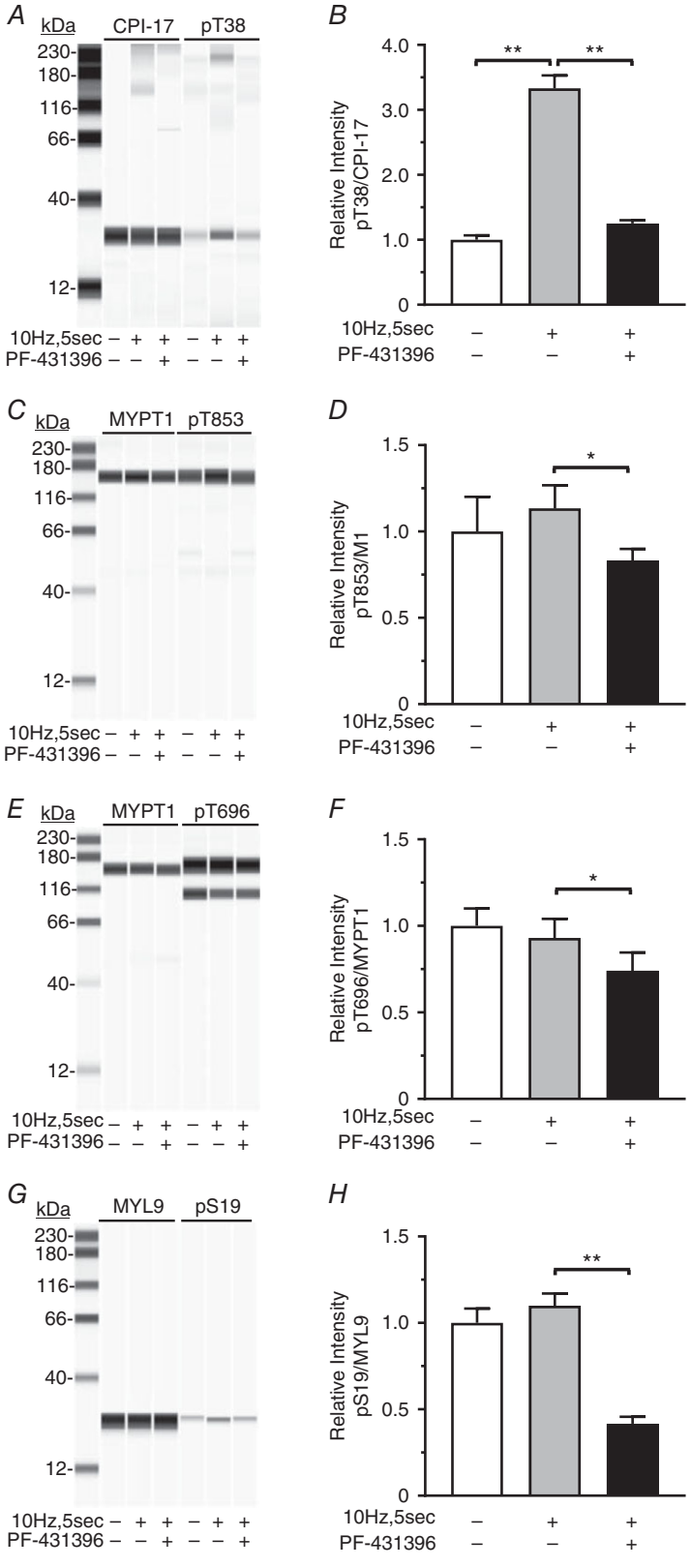

Figure 6. Effects of PF-431396 on EFS-evoked CPI-17, MYPT1 and MYL9 phosphorylation
A, *C*, *E* and *G*, representative immunoblots of CPI-17 and pT38, 0.5 μg per lane (*A*), MYPT1 and pT853, 0.5 μg per lane (*C*), MYPT1 and pT696, 0.5 μg per lane (*E*), and MYL9 and pS19, 0.5 μg per lane (*G*), from unstimulated and 10 Hz, 5 s EFS gastric fundus smooth muscles in the absence or presence of 0.3 μM PF-431396. *B*, *D*, *F* and *H*, the mean ± SD of the area under the peak intensity ratios for pT38:CPI-17 ($n = 3$) (*B*), pT853:MYPT1 ($n = 3$) (*D*), pT696:MYPT1 ($n = 3$) (*F*) and pS19:MYL9 ($n = 3$) (*H*), from unstimulated and 10 Hz, 5 s EFS muscles in the absence or presence of 0.3 μM PF-431396. $^*P < 0.05$, $^{**}P < 0.01$.

Discussion

In this study, we found that FAK phosphorylation is increased during EFS-evoked cholinergic neurotransmission contraction of gastric fundus smooth muscles. We also found that FAK activation in gastric fundus smooth muscles is Ca^{2+} independent, and likely involves mechanosensitive mechanisms. In addition, comparing the Pyk2 band intensities in Fig. 1*C* and *E* from gastric fundus muscles and liver suggests that FAK expression is higher than Pyk2 expression in gastric fundus muscles, but this could also be due to differences between the antibodies used for FAK and Pyk2 detection. These findings are different from the findings in vascular smooth muscles, in which Pyk2 autophosphorylation is significantly increased during contraction (Ohanian *et al.* 2005; Ying *et al.* 2009; Mills *et al.* 2015*a*). However, it has been reported that FAK phosphorylation is increased in bladder smooth muscles in response to KCl- or carbachol-induced contraction (Tsai *et al.* 2012). In tracheal smooth muscles, KCl- or carbachol-induced contractions increase FAK phosphorylation, and increases in force, intracellular Ca^{2+}, and MYL9 phosphorylation are inhibited by antisense knock-down of FAK expression (Mehta & Gunst, 1999). Contractile agonists increase FAK phosphorylation in hyperplastic human prostate smooth muscle, and the contractile responses are decreased by FAK inhibitors (Kunit *et al.* 2014).

PF-431396 has been shown to inhibit FAK and Pyk2 with similar IC_{50} values (Han *et al.* 2009). However, since we found that Pyk2 expression appears to be lower than FAK, and Pyk2 phosphorylation was barely detectable and not increased during contraction (Fig. 1), we used PF-431396 to inhibit FAK phosphorylation. Our dose–response studies showed that 0.1 μM PF-431396 reduced the basal level of FAK phosphorylation by 90%, with almost complete loss of FAK Y397 phosphorylation at 0.3 μM. There was no effect on basal tone of 0.3 μM PF-431396, while 1 and 3 μM PF-431396 significantly reduced basal tone (Fig. 2). These findings indicate the effect of 0.3 μM PF-431396 on contraction is likely due to inhibition of FAK phosphorylation, and not due to off-target effects of the compound. In fact, we found that 0.3 μM PF-431396 blocked the EFS-evoked increase in FAK Y397 phosphorylation, reduced Y397 phosphorylation below the basal level, and significantly inhibited EFS-induced contractions (Fig. 3), suggesting an

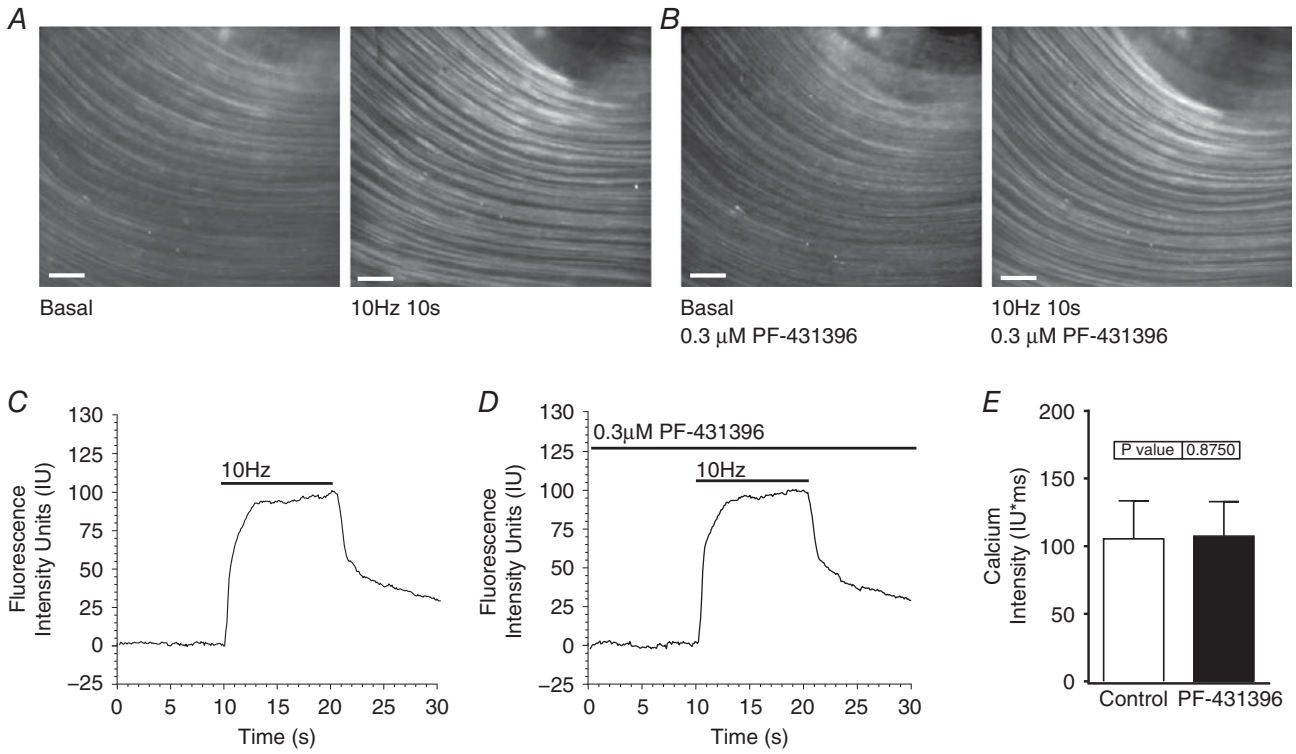

Figure 7. PF-431396 does not inhibit EFS-evoked Ca^{2+} influx into gastric fundus smooth muscle cells
A and *B*, representative images of the Cal-520 fluorescence evoked by 10 Hz, 10 s EFS of gastric fundus smooth muscles in the presence of 100 μM L-NAME and 1 μM MRS2500, in the absence (*A*) or presence (*B*) of 0.3 μM PF-431396 (scale bar: 200 μm). *C* and *D*, representative traces of the fluorescence intensity values evoked by 10 Hz, 10 s EFS of fundus smooth muscles in the absence (*C*) or presence (*D*) of 0.3 μM PF-431396. *E*, the mean ± SD of the area under the curve (AUC) of the Ca^{2+} intensity units measured from fundus muscle tissues during 10 Hz, 10 s EFS in the absence or presence of 0.3 μM PF-431396 ($n = 5$).

important role for FAK in gastric fundus smooth muscle contractions.

Gastric smooth muscles are composed of several populations of different cell types, all of which are important for muscle function (Sanders *et al.* 2012). Thus, to determine that FAK Y397 phosphorylation is increased in smooth muscle cells in response to cholinergic stimulation, we examined whether the muscarinic receptor blocker atropine would block the increase in FAK Y397 phosphorylation. We found that atropine blocked the EFS-evoked contractions, indicating a post-junctional loss of cholinergic signalling (Fig. 4). We found that atropine also blocked the increase in FAK Y397 phosphorylation in response to EFS-evoked cholinergic neurotransmission, indicating that FAK Y397 phosphorylation is increased in post-junctional cells, such as smooth muscle cells. It is interesting that atropine blocked the EFS-evoked increase in FAK Y397 phosphorylation, but did not reduce the level of pY397 below the basal level (Fig. 4*D*), as PF-431396 did (Fig. 3*D*). These findings suggest that PF-431396 inhibited basal FAK activity, and also inhibited the EFS-evoked increase in FAK activity. In contrast, the finding that atropine did not reduce the level of Y397 below the basal level suggests that basal FAK phosphorylation is maintained by a mechanism independent of muscarinic receptor activity.

In mouse gastric fundus smooth muscles, networks of interstitial cells of Cajal (ICC) and platelet-derived growth factor receptor α (PDGFRα) positive cells are also present post-junctionally (Sanders *et al.* 2014). FAK expression has been detected in mouse colon ICC and PDGFRα^+ cells by transcriptome analysis (Lee *et al.* 2015). To further show that FAK Y397 phosphorylation occurs in smooth muscle cells, we investigated the effects of high K^+-induced depolarization and contraction on FAK phosphorylation. High extracellular K^+ contracted gastric fundus smooth muscle strips and increased FAK Y397 phosphorylation, which were both inhibited by 0.3 μM PF-431396 (Fig. 5), further showing that FAK is activated in fundus smooth muscle cells. These findings provide additional evidence that FAK Y397 phosphorylation and inhibition of FAK Y397 phosphorylation occurs in smooth muscle cells, although these findings do not preclude changes in FAK phosphorylation also occurring in other cell types.

Pyk2 is a Ca^{2+}-stimulated protein tyrosine kinase, and in caudal artery smooth muscle cells, Pyk2 is activated by membrane depolarization and voltage-dependent Ca^{2+} influx resulting in RhoA activation, leading to MYPT1 and MYL9 phosphorylation and MLCP inhibition (Mills *et al.* 2015*a*). However, in gastric fundus smooth muscles, the involvement of RhoA and ROCK2 in MYPT1 phosphorylation by voltage-dependent Ca^{2+} influx is less likely, based on our findings that EFS-evoked cholinergic contractions do not increase MYPT1 T853 phosphorylation (Bhetwal *et al.* 2013). We found that in gastric fundus muscles, only CPI-17 T38 phosphorylation is increased by voltage-dependent Ca^{2+} influx, and this phosphorylation is inhibited by PKC inhibitors (Bhetwal *et al.* 2013). The findings of Mills *et al.* showing that MYPT1 phosphorylation is sensitive to Pyk2 inhibition led us to examine whether CPI-17 phosphorylation is sensitive to FAK inhibition in gastric fundus smooth muscles.

We found that PF-431396 significantly inhibited the increase in CPI-17 T38 phosphorylation evoked by 10 Hz, 5 s EFS. These findings suggest that FAK activity is necessary for PKC activation and CPI-17 T38

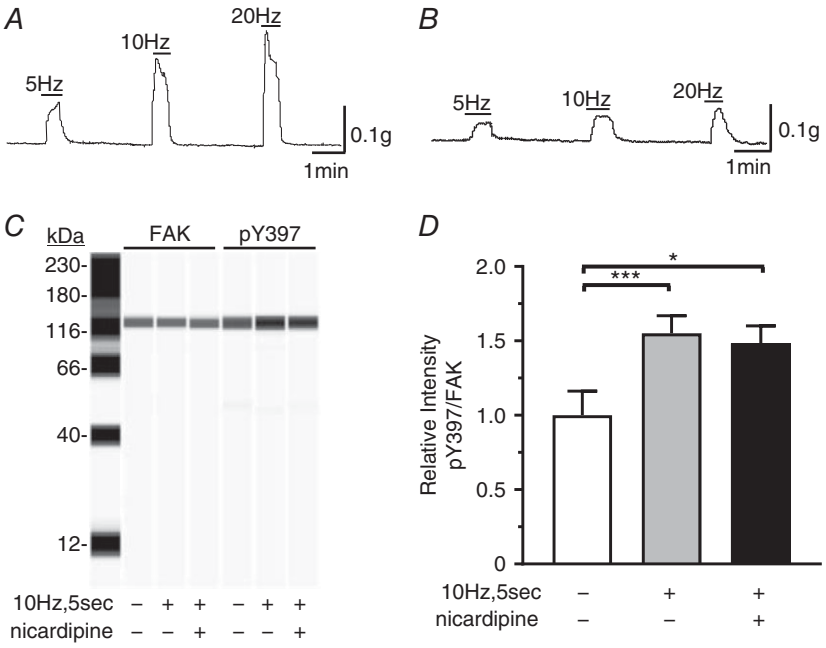

Figure 8. Nicardipine does not inhibit the EFS-evoked increase in FAK pY397 phosphorylation
A and *B*, representative traces of the contractile response of gastric fundus smooth muscles to 30 s of 5, 10 or 20 Hz EFS without (*A*) or with (*B*) 1 μM nicardipine in the presence of 100 μM L-NAME and 1 μM MRS2500 ($n = 3$). *C*, representative immuno-blot of FAK and pY397 from unstimulated and 10 Hz, 5 s EFS muscles in the absence or presence of 1 μM nicardipine; 0.5 μg per lane. *D*, the mean ± SD of pY397:FAK area under the peak intensity ratios from unstimulated and 10 Hz, 5 s EFS muscles in the absence or presence of 1 μM nicardipine ($n = 3$). $^*P < 0.05$, $^{***}P < 0.005$.

phosphorylation by EFS in gastric fundus smooth muscles. Further studies are required to determine whether FAK or a Src family kinase regulated by FAK phosphorylates PKC in murine gastric fundus smooth muscles. Interestingly, we found that MYPT1 T696 and T853 phosphorylation were also reduced by PF-431396. We previously found that MYPT1 T853 phosphorylation in gastric fundus muscles is sensitive to ROCK inhibition, suggesting that ROCK is the major kinase for T853 phosphorylation (Bhetwal *et al.* 2011). In contrast, we found that MYPT1 T696 phosphorylation is reduced by either nicardipine or a ROCK inhibitor, suggesting that MYPT1 T696 may be regulated by dual phosphorylation (Bhetwal *et al.* 2011). Thus, whether the decrease in MYPT1 T696 and T853 phosphorylation by PF-431396 is due to inhibition of FAK activation upstream of the RhoA/ROCK pathway, as reported for caudal arteries, is unclear (Mills *et al.* 2015*b*).

Conflicting reports describe activation or inhibition of L-type Ca^{2+} channel activity in smooth muscles by tyrosine kinases (Katsube *et al.* 1998; Wijetunge *et al.* 2000; Bogdelis *et al.* 2011). In addition, it is not uncommon for kinase inhibitors to have off-target effects on ion channels (Son *et al.* 2013). Thus, we used the fluorescent Ca^{2+} indicator dye Cal-520 to measure the EFS-evoked Ca^{2+} influx into gastric fundus smooth muscle cells. The levels and extent of the EFS-evoked Ca^{2+} influx

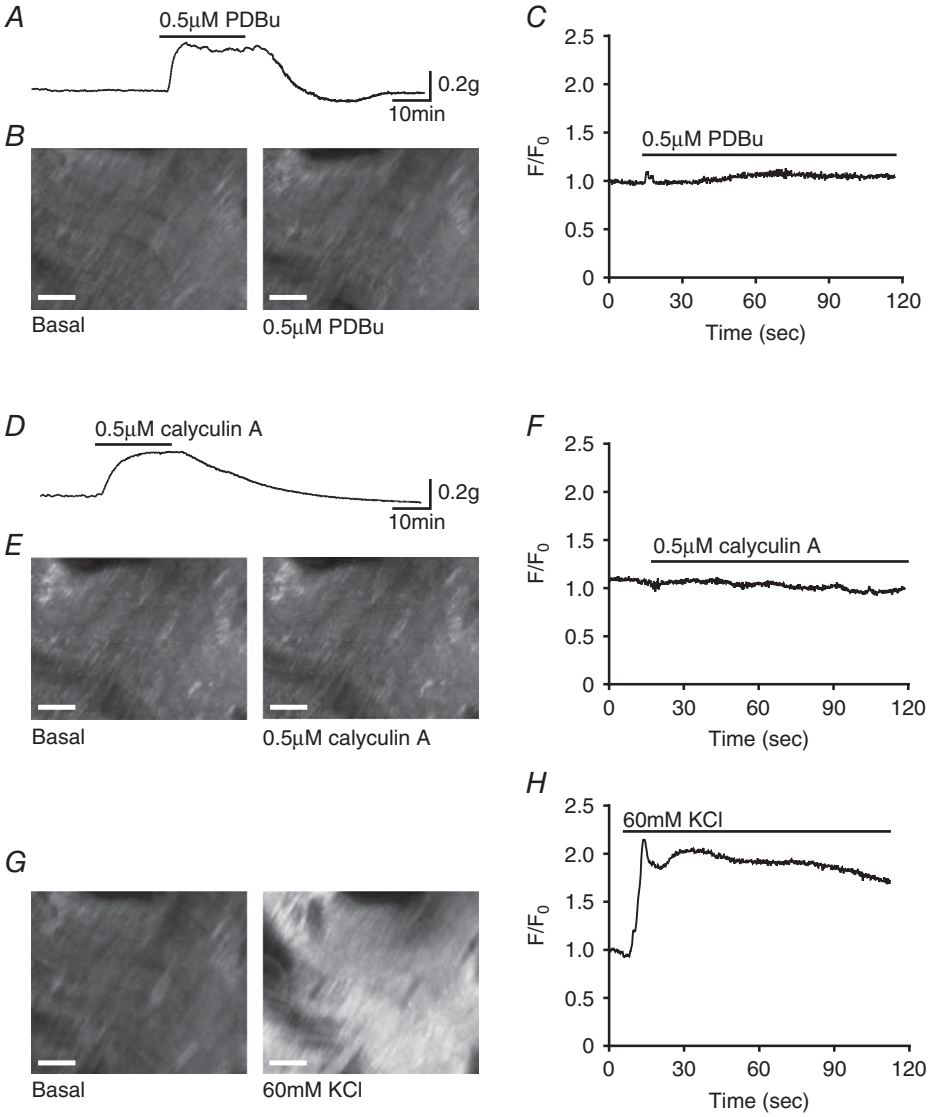

Figure 9. PDBu and calyculin A contract gastric fundus smooth muscles in a Ca^{2+}-independent manner
A–C, representative trace of the contractile response (*A*), image (*B*) and trace (*C*) of the GCaMP3 fluorescence evoked by 0.5 μM PDBu. *D–F*, representative trace of the contractile response (*D*), image (*E*) and trace (*F*) of the GCaMP3 fluorescence evoked by 0.5 μM calyculin A. *G* and *H*, representative image (*G*) and trace (*H*) of the GCaMP3 fluorescence evoked by 60 mM KCl (scale bar: μm). Tetrodotoxin (0.3 mM) was present in the myobaths ($n = 3$).

into smooth muscles in the absence or presence of PF-431396 were similar, strongly suggesting that the effects of PF-431396 on contraction, and on the phosphorylation of FAK Y397, CPI-17 T38, MYPT1 T696 and T853, and MYL9 S19 are due to FAK inhibition, and not due to inhibition of EFS-evoked Ca^{2+} influx. Although Ca^{2+} influx was not affected by PF-431396, MYL9 S19 phosphorylation was significantly decreased by PF-431396 treatment. This may be due to the inhibition of the increase in CPI-17 phosphorylation, and the decrease in MYPT1 phosphorylation by PF-431396. MLCP is known to be less inhibited, and thus more active, when CPI-17 and MYPT1 phosphorylation is reduced, resulting in antagonism of MYL9 phosphorylation by myosin light chain kinase during the EFS-induced Ca^{2+} influx (Gao *et al.* 2013).

The results of Figs 3 and 7 show that EFS of cholinergic neurons increases FAK phosphorylation and Ca^{2+} influx into smooth muscle cells, respectively. Although FAK and Pyk2 share domain structures and sequence homology, the FERM domain of Pyk2, but not the FAK FERM domain, binds to calmodulin in a Ca^{2+}-dependent manner (Kohno *et al.* 2008; Schaller, 2008). Our finding in Fig. 8 that the increase in FAK Y397 phosphorylation is nicardipine-insensitive suggests that Ca^{2+} influx is not involved in FAK activation in response to contraction of gastric fundus smooth muscles. Thus, to further examine the mechanisms of activation of FAK during contraction, we used PDBu or calyculin A to contract the gastric fundus smooth muscles in a Ca^{2+}-independent manner (Ishihara *et al.* 1989; Throckmorton *et al.* 1998; Dougherty *et al.* 2014). Figures 9 and 10 show that PDBu or calyculin A treatment contracted the muscle strips and increased FAK Y397 phosphorylation, with no corresponding increase in cytosolic Ca^{2+}, providing evidence that FAK responds to the mechanical stimuli associated with contraction. These findings are similar to the findings that during the contraction of tracheal smooth muscles, FAK is activated independently of Ca^{2+} influx (Tang & Gunst, 2001; Gunst *et al.* 2003). Although PKC has been implicated in activating FAK in several cell types (Fogh *et al.* 2014), our finding that FAK inhibition prevented the EFS-induced increase in CPI-17 phosphorylation suggests that FAK activation is upstream of PKC, and further suggests that FAK activity is required for PKC activation and CPI-17 phosphorylation. Additional studies are required to determine how mechanical signalling activates FAK in gastric fundus smooth muscle cells.

In conclusion, our results support a role for FAK in regulating Ca^{2+} sensitization mechanisms during gastric fundus smooth muscle contractions in response

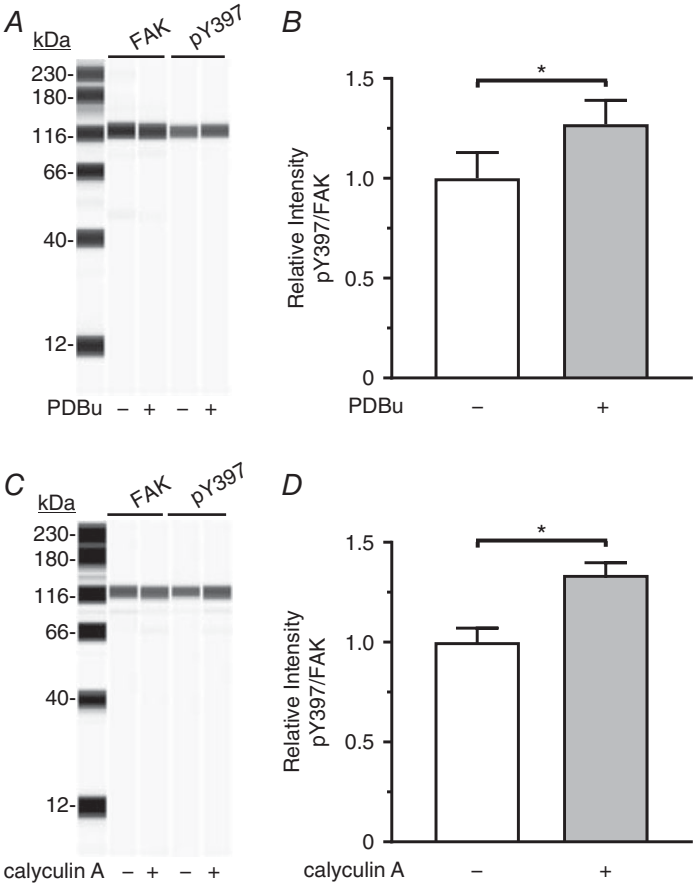

Figure 10. PDBu and calyculin A increase FAK Y397 phosphorylation
A and *C*, representative immunoblots of FAK and pY397 from unstimulated and 0.5 μM PDBu stimulated (*A*), and unstimulated and 0.5 μM calyculin A stimulated (*C*) gastric fundus muscles; 0.5 μg per lane. *B* and *D*, the mean ratios ± SD of the pY397:FAK area under the peak intensity ratios from unstimulated and 0.5 μM PDBu stimulated (*B*), and unstimulated and 0.5 μM calyculin A stimulated (*D*) gastric fundus muscles ($n = 3$). *$P < 0.05$.

to EFS-evoked cholinergic motor signalling. Previously, Tyr phosphorylation of FAK and recruitment to focal adhesions via complex formation with integrins have been shown to occur during contraction in smooth muscles (Ohanian *et al.* 2015; Tang, 2015). These interactions are thought to facilitate the polymerization of cortical actin filaments to stabilize adhesion complexes in the membrane, allowing the force generated by myofilament activation to be transmitted to the connective tissue of the extracellular matrix (Mehta & Gunst, 1999; Chen *et al.* 2015; Mills *et al.* 2015*b*). The present work introduces an additional role for FAK in gastric fundus smooth muscle contractile function, by an apparent involvement in the regulation of CPI-17 and also MYPT1 phosphorylation.

References

Baker SA, Drumm BT, Saur D, Hennig GW, Ward SM & Sanders KM (2016). Spontaneous Ca^{2+} transients in interstitial cells of Cajal located within the deep muscular plexus of the murine small intestine. *J Physiol* **594**, 3317–3338.

Bhetwal BP, An CL, Fisher SA & Perrino BA (2011). Regulation of basal LC20 phosphorylation by MYPT1 and CPI-17 in murine gastric antrum, gastric fundus, and proximal colon smooth muscles. *Neurogastroenterol Motil* **23**, e425–e436.

Bhetwal BP, Sanders KM, An C, Trappanese DM, Moreland RS & Perrino BA (2013). Ca^{2+} sensitization pathways accessed by cholinergic neurotransmission in the murine gastric fundus. *J Physiol* **591**, 2971–2986.

Bogdelis A, Treinys R, Stankevičius E, Jurevičius J & Skeberdis VA (2011). Src family protein tyrosine kinases modulate L-type calcium current in human atrial myocytes. *Biochem Biophys Res Commun* **413**, 116–121.

Chen CP, Chen X, Qiao YN, Wang P, He WQ, Zhang CH, Zhao W, Gao YQ, Chen C, Tao T, Sun J, Wang Y, Gao N, Kamm KE, Stull JT & Zhu MS (2015). In vivo roles for myosin phosphatase targeting subunit-1 phosphorylation sites T694 and T852 in bladder smooth muscle contraction. *J Physiol* **593**, 681–700.

Chien PT-Y, Lin C-C, Hsiao L-D & Yang C-M (2015). c-Src/Pyk2/EGFR/PI3K/Akt/CREB-activated pathway contributes to human cardiomyocyte hypertrophy: Role of COX-2 induction. *Mol Cell Endocrinol* **409**, 59–72.

Dougherty PJ, Nepiyushchikh ZV, Chakraborty S, Wang W, Davis MJ, Zawieja DC & Muthuchamy M (2014). PKC activation increases Ca^{2+} sensitivity of permeabilized lymphatic muscle via myosin light chain 20 phosphorylation-dependent and -independent mechanisms. *Am J Physiol Heart Circulat Physiol* **306**, H674–H683.

Fogh BS, Multhaupt HAB & Couchman JR (2014). Protein kinase C, focal adhesions and the regulation of cell migration. *J Histochem Cytochem* **62**, 172–184.

Gao N, Huang J, He W, Zhu M, Kamm KE & Stull JT (2013). Signaling through myosin light chain kinase in smooth muscles. *J Biol Chem* **288**, 7596–7605.

Grassie ME, Moffat LD, Walsh MP & MacDonald JA (2011). The myosin phosphatase targeting protein (MYPT) family: a regulated mechanism for achieving substrate specificity of the catalytic subunit of protein phosphatase type 1δ. *Arch Biochem Biophys* **510**, 147–159.

Grundy D (2015). Principles and standards for reporting animal experiments in *The Journal of Physiology* and *Experimental Physiology*. *J Physiol* **593**, 2547–2549.

Gunst SJ, Tang DD & Opazo Saez A (2003). Cytoskeletal remodeling of the airway smooth muscle cell: a mechanism for adaptation to mechanical forces in the lung. *Resp Physiol Neurobiol* **137**, 151–168.

Han S, Mistry A, Chang JS, Cunningham D, Griffor M, Bonnette PC, Wang H, Chrunyk BA, Aspnes GE, Walker DP, Brosius AD & Buckbinder L (2009). Structural characterization of proline-rich tyrosine kinase 2 (PYK2) reveals a unique (DFG-out) conformation and enables inhibitor design. *J Biol Chem* **284**, 13193–13201.

Hartshorne DJ, Ito M & Erdodi F (2004). Role of protein phosphatase type 1 in contractile functions: myosin phosphatase. *J Biol Chem* **279**, 37211–37214.

He WQ, Peng YJ, Zhang WC, Lv N, Tang J, Chen C, Zhang CH, Gao S, Chen HQ, Zhi G, Feil R, Kamm KE, Stull JT, Gao X & Zhu MS (2008). Myosin light chain kinase is central to smooth muscle contraction and required for gastrointestinal motility in mice. *Gastroenterology* **135**, 610–620.

Hirano K (2007). Current topics in the regulatory mechanism underlying the Ca^{2+} sensitization of the contractile apparatus in vascular smooth muscle. *J Pharmacol Sci* **104**, 109–115.

Horowitz A, Menice CB, Laporte R & Morgan KG (1996). Mechanisms of smooth muscle contraction. *Physiol Rev* **76**, 967–1003.

Ishihara H, Ozaki H, Sato K, Hori M, Karaki H, Watabe S, Kato Y, Fusetani N, Hashimoto K & Uemura D (1989). Calcium-independent activation of contractile apparatus in smooth muscle by calyculin-A. *J Pharmacol Exp Ther* **250**, 388–396.

Katsube Y, Yokoshiki H, Nguyen L, Yamamoto M & Sperelakis N (1998). Inhibition of Ca^{2+} current in neonatal and adult rat ventricular myocytes by the tyrosine kinase inhibitor, genistein. *Eur J Pharmacol* **345**, 309–314.

Khasnis M, Nakatomi A, Gumpper K & Eto M (2014). Reconstituted human myosin light chain phosphatase reveals distinct roles of two inhibitory phosphorylation sites of the regulatory subunit, MYPT1. *Biochem* **53**, 2701–2709.

Kim M, Cho SY, Han IS, Koh SD & Perrino BA (2005). CaM kinase II and phospholamban contribute to caffeine-induced relaxation of murine gastric fundus smooth muscle. *Am J Physiol Cell Physiol* **288**, C1202–C1210.

Kohno T, Matsuda E, Sasaki H & Sasaki T (2008). Protein-tyrosine kinase CAKβ/PYK2 is activated by binding Ca^{2+}/calmodulin to FERM F2 α2 helix and thus forming its dimer. *Biochem J* **410**, 513–523.

Kunit T, Gratzke C, Schreiber A, Strittmatter F, Waidelich R, Rutz B, Loidl W, Andersson K-E, Stief CG & Hennenberg M (2014). Inhibition of smooth muscle force generation by focal adhesion kinase inhibitors in the hyperplastic human prostate. *Am J Physiol Renal Physiol* **307**, F823–F832.

Lee MY, Park C, Berent RM, Park PJ, Fuchs R, Syn H, Chin A, Townsend J, Benson CC, Redelman D, Shen T-W, Park JK, Miano JM, Sanders KM & Ro S (2015). Smooth muscle cell genome browser: Enabling the identification of novel serum response factor target genes. *PLoS One* **10**, e0133751.

Luo DY, Wazir R, Tian Y, Yue X, Wei TQ & Wang KJ (2013). Integrin αv mediates contractility whereas integrin α4 regulates proliferation of human bladder smooth muscle cells via FAK pathway under physiological stretch. *J Urol* **190**, 1421–1429.

Matsumura F & Hartshorne DJ (2008). Myosin phosphatase target subunit: many roles in cell function. *Biochem Biophys Res Comm* **369**, 149–156.

Mehta D & Gunst SJ (1999). Actin polymerization stimulated by contractile activation regulates force development in canine tracheal smooth muscle. *J Physiol* **519**, 829–840.

Mills RD, Mita M, Nakagawa Ji, Shoji M, Sutherland C & Walsh MP (2015*a*). A role for the tyrosine kinase Pyk2 in depolarization-induced contraction of vascular smooth muscle. *J Biol Chem* **290**, 8677–8692.

Mills RD, Mita M & Walsh MP (2015*b*). A role for the Ca^{2+}-dependent tyrosine kinase Pyk2 in tonic depolarization-induced vascular smooth muscle contraction. *J Muscle Res Cell Motil* **36**, 479–489.

Mizuno Y, Isotani E, Huang J, Ding H, Stull JT & Kamm KE (2008). Myosin light chain kinase activation and calcium sensitization in smooth muscle in vivo. *Am J Physiol Cell Physiol* **295**, C358–C364.

Ohanian J, Pieri M & Ohanian V (2015). Non-receptor tyrosine kinases and the actin cytoskeleton in contractile vascular smooth muscle. *J Physiol* **593**, 3807–3814.

Ohanian V, Gatfield K & Ohanian J (2005). Role of the actin cytoskeleton in G-protein-coupled receptor activation of PYK2 and paxillin in vascular smooth muscle. *Hypertension* **46**, 93–99.

Sanders KM, Koh SD, Ro S & Ward SM (2012). Regulation of gastrointestinal motility—insights from smooth muscle biology. *Nat Rev Gastroenterol Hepatol* **9**, 633–645.

Sanders KM, Ward SM & Koh SD (2014). Interstitial cells: regulators of smooth muscle function. *Physiol Rev* **94**, 859–907.

Saphirstein RJ, Gao YZ, Jensen MH, Gallant CM, Vetterkind S, Moore JR & Morgan KG (2013). The focal adhesion: a regulated component of aortic stiffness. *PLoS One* **8**, e62461.

Schaller MD (2008). Calcium-dependent Pyk2 activation: a role for calmodulin? *Biochem J* **410**, e3–e4.

Schindelin J, Arganda-Carreras I, Frise E, Kaynig V, Longair M, Pietzsch T, Preibisch S, Rueden C, Saalfeld S, Schmid B, Tinevez JY, White DJ, Hartenstein V, Eliceiri K, Tomancak P & Cardona A (2012). Fiji: an open-source platform for biological-image analysis. *Nat Methods* **9**, 676–682.

Somlyo AP & Somlyo AV (2003). Ca^{2+} sensitivity of smooth muscle and nonmuscle myosin II: modulated by G proteins, kinases, and myosin phosphatase. *Physiol Rev* **83**, 1325–1358.

Son Y, Park H, Firth A & Park W (2013). Side-effects of protein kinase inhibitors on ion channels. *J Biosci* **38**, 937–949.

Tang DD (2015). Critical role of actin-associated proteins in smooth muscle contraction, cell proliferation, airway hyperresponsiveness and airway remodeling. *Resp Rese* **16**, 134.

Tang DD & Gunst SJ (2001). Depletion of focal adhesion kinase by antisense depresses contractile activation of smooth muscle. *Am J Physiol Cell Physiol* **280**, C874–C883.

Throckmorton DC, Packer CS & Brophy CM (1998). Protein kinase C activation during Ca^{2+}-independent vascular smooth muscle contraction. *J Surg Res* **78**, 48–53.

Tsai MH, Chang AN, Huang J, He W, Sweeney HL, Zhu M, Kamm KE & Stull JT (2014). Constitutive phosphorylation of myosin phosphatase targeting subunit-1 in smooth muscle. *J Physiol* **592**, 3031–3051.

Tsai MH, Kamm KE & Stull JT (2012). Signalling to contractile proteins by muscarinic and purinergic pathways in neurally stimulated bladder smooth muscle. *J Physiol* **590**, 5107–5121.

Wijetunge S, Lymn JS & Hughes AD (2000). Effects of protein tyrosine kinase inhibitors on voltage-operated calcium channel currents in vascular smooth muscle cells and $pp60^{c\text{-}src}$ kinase activity. *Br J Pharmacol* **129**, 1347–1354.

Ying Z, Giachini FRC, Tostes RC & Webb RC (2009). Salicylates dilate blood vessels through inhibiting PYK2-mediated RhoA/Rho-kinase activation. *Cardiovasc Res* **83**, 155–162.

Yu Y, Ross SA, Halseth AE, Hollenbach PW, Hill RJ, Gulve EA & Bond BR (2005). Role of PYK2 in the development of obesity and insulin resistance. *Biochem Biophys Res Commun* **334**, 1085–1091.

Additional information

Competing interests

The authors declare no competing interests.

Author contributions

B.A.P., Y.X. and K.H.H. designed the experiments, analysed the data, wrote the manuscript and contributed to the discussion and review of the manuscript. K.H.H., R.D.C. and N.G. performed the Ca^{2+} imaging experiments and analysed the data. W.L. performed and analysed the PDBu experiments. Y.X. performed all the other experiments and analysed the data. All authors have read and approved the final version of this manuscript and agree to be accountable for all aspects of the work in ensuring that questions related to the accuracy or integrity of any part of the work are appropriately investigated and resolved. All persons designated as authors qualify for authorship, and all those who qualify for authorship are listed.

Funding

This work was supported by a Takeda Pharmaceuticals Innovation Centre Grant to B.A.P., and in part by a Mick Hitchcock Graduate Student Scholarship to Y.X.

Acknowledgements

We thank Sang Don Koh for his assistance with the interpretation and analysis of the Ca^{2+} imaging experiments.